Estuarine, Coastal and Shelf Science 83 (2009) 148–158

Contents lists available at ScienceDirect

Estuarine, Coastal and Shelf Science

journal homepage: www.elsevier.com/locate/ecss

# Long-term numerical evolution of the nitrogen bulk content in the Mediterranean Sea

G. Crispi*, M. Pacciaroni

*Istituto Nazionale di Oceanografia e di Geofisica Sperimentale, Borgo Grotta Gigante 42/c, 34010 Sgonico, Trieste, Italy*

ARTICLE INFO

*Article history:*
Received 12 October 2007
Accepted 7 December 2007
Available online 12 February 2008

*Keywords:*
nitrogen
biogeochemical modelling
biomass
ecosystem stability
Mediterranean Sea

ABSTRACT

The behavior of the Mediterranean ecosystem in response to realistic riverine inputs and dissolved matter exchange is investigated. The strategy is to evaluate the stability of the ecosystem subjected to various atmospheric inputs.

For this purpose, we employ a generic three-dimensional biogeochemical description, based on inorganic nitrogen, phytoplankton, zooplankton and detritus. The model is developed for the oligotrophic Mediterranean Sea at $1/8^\circ \times 1/8^\circ$ horizontal resolution.

The total nitrogen content in the Mediterranean Sea remains stable, with an overall annual loss of approximately $150 \times 10^3$ ton N year$^{-1}$, attributable to further diffused terrestrial discharges of nitrogen along the central and the northwestern coasts.

The total contents of nitrogen in Western and Eastern Mediterranean exhibit opposite tendency in the intermediate layers below 180 m, increasing in the former and decreasing in the latter. The upper euphotic layer of the Western Mediterranean over a long time frame has high total nitrogen content, more than 600 mmol N m$^{-2}$, compared with the Eastern Mediterranean, which is less than 250 mmol N m$^{-2}$, showing the development of different typical trophic regimes from the initial homogeneous status.

The vertically integrated chlorophyll concentrations evidence at the end of the long-term simulation a clear west–east decreasing gradient; the average of the Western Mediterranean turns out twice the amount of the Eastern Mediterranean.



## 1. Introduction

The study of the Mediterranean ecosystem is complex, which is attributed to the superposition of different effects. Parts of these have features common with the World Ocean, whereas other parts have specific features, first of all nutrient-depleted regime and its influence on oligotrophy and relative abundances of species. The origin of this regime stems from the various physical processes that occur in the basin, with many consequent outcomes from the viewpoints of geochemistry, life inside the sea, and ecology. The points to be addressed in synthetic approaches are described as follows.

The upper layer of Mediterranean has its main variability at the seasonal scale due to the atmospheric forcings and the permanent and recurrent gyres of the sub-basins. The thermocline is seasonal, with absence of permanent thermocline. Thus, the vertical structure in the Mediterranean Sea is very different from that of the northeastern Atlantic counterpart, but with some similarities with the anticyclonic Sargasso Sea, due to the annual winter breakdown of the seasonal thermocline with consequent mixing of nutrient to deeper depths (Dugdale and Goering, 1967).

The morphology of the Mediterranean continental shelves shows the following significant characteristics. The northwestern shelf tends to be narrow with steep continental slope, full of submarine canyons. The Adriatic Sea, comprising a relatively broad shallow shelf, and the Aegean Sea, containing intershelf basins, complete the list of the three main broad shelves. As a matter of fact, changes in terrestrial and atmospheric inputs to Mediterranean shelves in the form of nutrients, particulate and dissolved matter, in the 1970s and 1980s, have induced modifications in the ambience of pelagic ecosystem (Bethoux et al., 1992).

As a result of freshwater riverine inputs in limited amounts, evaporation exceeds precipitation, resulting in high salinities in all the Mediterranean water masses. In order to balance the net loss of water from evaporation, surface water from the Eastern Atlantic flows into the Mediterranean, resulting in easterly surface

* Corresponding author.
*E-mail address:* gcrispi@ogs.trieste.it (G. Crispi).

0272-7714/$ – see front matter © 2008 Elsevier Ltd. All rights reserved.
doi:10.1016/j.ecss.2007.12.015

circulation. The evaporation excess increases the salinity, promoting sinking to intermediate depths, which is the source of westerly interior circulation. Analogously, accumulation of high concentration of nutrients in the deep-water is prevented by continuous exchange of water through the main Straits, giving relatively short residence times of the order of 100 years.

The reason for the oligotrophy of the Mediterranean is thence explained as a response to the exiguity of nutrient inputs and to the negative thermohaline circulation, with the precise biogeochemical mechanism, which controls oligotrophy, being the biological pump (Crispi et al., 2001). This biophysical assessment has been given both in terms of nitrogen and phosphorus, taking into account the appropriate recycling rates of these two elements. Anyway, these results have been obtained by means of a parsimonious box model, maintaining unresolved regional impacts of realistic aeolian and terrestrial inputs.

Nitrogen is considered a key nutrient for understanding the inner processes associated with nutrient flow in the Mediterranean since its various fractions represent different aspects of processes occurring in the ecosystem (Dugdale and Wilkerson, 1988). In fact, silicate does not significantly limit the functioning of the ecosystem, because of its abundance in the euphotic zone. Whereas, phosphate shows no similar fractionation and moreover gives rise to chemical processes, possibly at the base of this oligotrophic state, via the precipitation of orthophosphate with iron contained in the dust from Sahara. Other chemical interactions occur between calcium carbonate and phosphate during formation of phosphorites and apatites, with possible association between vertical phosphate transport and occurrence of coccolithophorids in the Mediterranean.

The choice of nitrogen avoids the necessity for considering the above-mentioned peculiarities of the phosphorus cycle, and therefore nitrogen is selected as the limiting nutrient for this study, also with major coverage of the Mediterranean in terms of historical and recent data sets. Interactions and fractionation effects suggest the development of multi-nutrient ecosystem, whose implementation should fully resolve the carbon- and nutrient-linked cycles, addressing the concurrent nitrogen–phosphorus limitation in the competition occurring for these nutrients in phytoplankton and heterotrophic bacteria (Thingstad and Rassoulzadegan, 1995).

The Mediterranean geochemical cycling of nutrients depends on the three following exchanges with external systems: the inflow and outflow with the Atlantic Ocean, influencing the redistribution paths of the saline intermediate water masses produced in the Levantine Basin, which are important to trigger deep-water convection (Wu and Haines, 1996); the atmospheric inputs, which modify the upper layer concentrations in terms of the different oligoelements; the inflow of freshwater by the main rivers and Bosphorus Strait, prevalently affecting coastal areas. These three facts determine: an oligotrophic ecosystem, a deep benthic system that cycles at low energy sill, with anomalous nutrient ratio with respect to the ratio in the World Ocean, described by Redfield et al. (1963).

This study addresses the development of a numerical description of the Mediterranean ecosystem, simulating, by means of a three-dimensional NPZD model, the above-mentioned factors as external loads of the biogeochemical dynamics. Its aim is to study the ecosystem stability, after recognition of the main trends and budgets on the basis of this biogeochemical modelling approach.

The overall system requires that all the variables are in dynamic balance and that on an average the total content is stable along the integration times. This part of refinement of the model is discussed in Section 2. Later, the results of the study are shown on a long-term basis and the conclusions are outlined.

## 2. Methods and data

### 2.1. Primitive equation model

The dynamics of the Mediterranean oligotrophic ecosystem is studied by coupling it with the Mediterranean basin circulation as simulated by MOM, general circulation model driven by high frequency forcing. This is the Geophysical Fluid Dynamics Laboratory Modular Ocean Model (Pacanowski et al., 1991), which is a finite difference formulation of the primitive equations governing ocean circulation.

These equations consist of the hydrostatic Navier–Stokes equations along with a nonlinear equation of state, which couples the two active tracers, temperature and salinity, to the fluid velocity.

The hydrodynamics is based on the following fully 3-D primitive equations in a spherical coordinate system ($\lambda$, $\varphi$, $z$), where $\lambda$ is longitude increasing eastward, $\varphi$ is latitude increasing northward, and $z$ is positive upward with zero defined at the ocean surface:

$$\frac{\partial \overline{v}}{\partial t} + (\overline{u}\cdot\nabla)\overline{v} + \overline{f}\times\overline{v} = -\frac{1}{\rho_0}\nabla_{\mathrm{H}} p - A_{\mathrm{H}}\nabla_{\mathrm{H}}^4\overline{v} + A_{\mathrm{V}}\frac{\partial^2\overline{v}}{\partial z^2} \tag{1}$$

$$\frac{\partial p}{\partial z} = -\rho g \tag{2}$$

$$\nabla\cdot\overline{u} = 0 \tag{3}$$

$$\frac{\partial T}{\partial t} + (\overline{u}\cdot\nabla)T = -K_{\mathrm{H}}\nabla_{\mathrm{H}}^4 T + K_{\mathrm{V}}\frac{\partial^2 T}{\partial z^2} + \alpha_{\mathrm{T}}(T - T_0) \tag{4}$$

$$\frac{\partial S}{\partial t} + (\overline{u}\cdot\nabla)S = -K_{\mathrm{H}}\nabla_{\mathrm{H}}^4 S + K_{\mathrm{V}}\frac{\partial^2 S}{\partial z^2} + \alpha_{\mathrm{S}}(S - S_0) \tag{5}$$

$$\rho = \rho(T, S, p) \tag{6}$$

In the preceding equations $\overline{v} = (v_\lambda, v_\varphi)$ and $w = v_z$ are the horizontal and vertical components of the velocity $\overline{u}$, $T$ and $S$ are the temperature and salinity, and $p$ and $\rho$ represent the pressure and density, respectively. The Coriolis parameter is given by $\overline{f} = 2\Omega \sin\varphi\overline{k}$, where $g$ is the gravity constant and $\overline{k}$ is the vertical unitary vector. $A_{\mathrm{H}}$ and $A_{\mathrm{V}}$ are the horizontal and vertical constant eddy viscosity coefficients, while $K_{\mathrm{H}}$ and $K_{\mathrm{V}}$ are the horizontal and vertical constant turbulent diffusion coefficients, respectively. Eqs. (4) and (5) are the equations for the potential temperature and salinity of the active tracers. The second term in (1), (4) and (5) is the advection operator in spherical coordinates and includes the three velocity components. Eq. (6) is the UNESCO (1981) equation of state for seawater.

In particular, the simulations reported here adopt MOM for the Mediterranean Sea plus a buffer zone representing the Atlantic inflow/outflow. The transport through the Strait of Gibraltar is parameterised in an extended area, where temperature and salinity are relaxed toward annual climatological fields.

The biharmonic horizontal eddy viscosity and diffusivity are $0.5\times10^{18}$ and $1.5\times10^{18}$ cm$^4$ s$^{-1}$, respectively. The vertical viscosity is 1.5 cm$^2$ s$^{-1}$ and the vertical diffusivity for physical tracers is 0.3 cm$^2$ s$^{-1}$.

The model is integrated throughout the entire Mediterranean basin, with a horizontal spatial discretization of 1/8° and a vertical resolution of 31 levels (Demirov and Pinardi, 2002). The vertical levels are unevenly spaced down to 4000 m, and the tracer values, temperature, salinity, and biogeochemical ones are placed at 5, 15, 30, 50, 70, 90, 120, 160, 200, 240, 280, 320, 360, 400, 440, 480, 520,

580, 660, 775, 925, 1150, 1450, 1750, 2050, 2350, 2650, 2950, 3250, 3550, 3850 m.

A standard convective adjustment procedure is applied, mixing the contents of two adjacent levels, up to $n_C$ times, when static instability appears in the water column. When instabilities are introduced in the biogeochemistry, the terms for biological sources and sinks are set to zero.

The $\alpha$ terms in Eqs. (4) and (5) are the Newtonian restoring terms that have values not equalling zero only in selected regions of the model. Both temperature and salinity have $\alpha_T$ and $\alpha_S$ equal to 1.0 day$^{-1}$.

Air–sea physical parameterizations account for the heat budget at the air–sea interface according to Roussenov et al. (1995). The surface heat forcing is computed in an interactive way with six-hourly atmospheric reanalysis fields from European Centre for Medium-Range Weather Forecasts and sea surface temperature from the model. The meteorological data used are the atmospheric temperature and humidity at 2 m, wind components at 10 m, and the percentage of the cloud cover. In the simulations reported here, perpetual year-long evolution is attained using the forcing data of 1998: after 31st December, the year cycles with data of 1st January of the 1998 data set.

The specification of salt fluxes at the sea surface is generally related to the problem of prescribing precipitation–evaporation values; however, the problem is solved by imposing the salinity structure at the first model level, as indicated by Eq. (5). The surface salinity boundary condition is a relaxation to climatological monthly mean values.

In the Mediterranean MOM model, the solid boundaries are non-slip and insulating for temperature and salinity. The bottom is free slip and insulating. Three-dimensional hydrodynamic Eqs. (1)–(6) with relevant boundary conditions are solved using a second-order finite difference method on the numerical B-grid, using 900 s as time step.

### 2.2. NPZD ecomodel

The 3-D coupling of the biochemical tracer with hydrodynamics and its parameterization are on the same grid of the Mediterranean circulation model, 1/8°, where the equations describing nitrogen uptake, grazing, and remineralization processes are integrated. The generic equation of the biochemical tracer $B$ with sea velocity field $\overline{u} = (u, v, w)$ is:

$$\frac{\partial B}{\partial t} + (\overline{u}\cdot\nabla)B = -K_H^B \nabla_H^4 B + K_V^B \frac{\partial^2 B}{\partial z^2} - w_B \frac{\partial B}{\partial z} + \left.\frac{\partial B}{\partial t}\right|_{SOURCE} \quad (7)$$

The ecological processes are described using NPZD model, in the order of inorganic nitrogen, $N$, phytoplankton, $P$, zooplankton, $Z$, and detritus, $D$, and consistently the description of the ecosystem has been set up in accordance with the requirements concerning the fluxes between the biochemical tracers.

The phytoplankton source–sink equation is given by the following expression:

$$\left.\frac{\partial P}{\partial t}\right|_{SOURCE} = G\frac{NP}{k_N + N} - dP - \gamma\frac{PZ}{k_P + P} \quad (8)$$

The uptake, $G$, has the form

$$G = G(T, z, t, N) = G_{max}\, e^{-k_T T} L_f(z,t) F_0(t) N_f(N) \quad (9)$$

where $G_{max}$ is the maximum growth rate and $k_T$ is the temperature coefficient; $L_f(z,t)$ is the light limitation function according to Steele (1962), given by the expression

$$L_f(z,t) = \frac{I_0(t)\, e^{-k_z z}}{I_{opt}} e^{1-\frac{I_0(t)\, e^{-k_z z}}{I_{opt}}}; \quad (10)$$

$F_0(t)$ is the photoperiod, i.e. the irradiance day length (Carrada et al., 1983):

$$F_0(t) = 0.5 - 0.125\cos\left(\frac{2\pi(\text{day}+10)}{365}\right); \quad (11)$$

and, finally, $N_f$ is the Michaelis–Menten formulation for the nitrogen limitation

$$N_f(N) = \frac{N}{k_N + N} \quad (12)$$

written in terms of the available inorganic nitrogen, $N$, and of the uptake half-saturation, $k_N$. All the limiting factors for the phytoplankton, as well as the mortality rate, are considered in the Mediterranean environment and are characteristic of the response to the light and nutrients present in the sea (Eppley et al., 1969; Sakshaug et al., 1989; Crispi et al., 2002).

The zooplankton specific flux is expressed as:

$$\left.\frac{\partial Z}{\partial t}\right|_{SOURCE} = \eta g - \delta Z = \eta\gamma\frac{PZ}{k_P + P} - \delta Z \quad (13)$$

Grazing is simulated through a second-order Holling function, where the parameters are kept fixed with all the ambient variability indicators, except for parameters with respect to density of the prey, phytoplankton, and the predator, generalized as zooplankton. The grazed biomass, $g$, is a total loss for phytoplankton compartment and partial source for zooplankton.

The parameters of this flux reflect the behavior of copepods (Fasham et al., 1990); the degradation fraction is an average of their detrital fraction of mortality, which is higher and is exported from the mixed layer via detritus sinking, and of their dissolved organic nitrogen fraction of excretion by zooplankton, which is lower and is recycled inside the mixed layer.

The above-mentioned five biochemical fluxes are closed in the model by the detritus remineralization and by the sloppy feeding which gives the amount of the egested phytoplankton.

Thus, the nitrate flux takes into account all the other biochemical variables as follows:

$$\left.\frac{\partial N}{\partial t}\right|_{SOURCE} = rD + (1-\alpha)\delta Z - G\frac{NP}{k_N + N} \quad (14)$$

Finally, the detritus chain describes the remaining part of the recycling of the nonliving organic matter, particulate and dissolved, produced by exogenous input, mortality processes and remineralization, all set as linear processes:

$$\left.\frac{\partial D}{\partial t}\right|_{SOURCE} = dP + (1-\eta)\gamma\frac{PZ}{k_P + P} + \alpha\delta Z - rD \quad (15)$$

All the biochemical parameters of Table 1 are chosen in the ranges described in the literature for oligotrophic environments. This permits to calibrate, considering selected results from different projects, the ecomodel values of detritus remineralization and sinking, $r$ and $w_D$, also given in Table 1.

The growth rates of phytoplankton are of the order of those measured in different oligotrophic sites (Eppley et al., 1969) and, moreover, this model is capable of recovering high frequency responses in relation to proper sampling of the forcing functions (Crispi et al., 2006). The overwintering exhibited by zooplankton is obtained without any recourse to feeding strategies and can be chosen as optimization target.

**Table 1**
List of the parameters of the biogeochemical model.

| Parameter | Definition | Value | Reference |
|---|---|---|---|
| $G_{max}$ ($s^{-1}$) | Maximum growth rate | $6.83 \times 10^{-6}$ | Eppley et al. (1969) |
| $k_T$ ($°C^{-1}$) | Temperature coefficient | $6.33 \times 10^{-2}$ | Eppley et al. (1969) |
| $k_z$ ($cm^{-1}$) | Light extinction coefficient | $3.4 \times 10^{-4}$ | Crispi et al. (2002) |
| $I_{opt}/I_0$ | Optimum light ratio | 0.5 | Steele (1962) |
| $k_N$ (μmol N $dm^{-3}$) | Uptake half-saturation | 0.25 | Crispi et al. (2002) |
| $d$ ($s^{-1}$) | Phytoplankton mortality | $5.55 \times 10^{-7}$ | Sakshaug et al. (1989) |
| $R_{NC}$ (μmol N (μmol C)$^{-1}$) | Nitrogen to carbon ratio in phytoplankton | 0.151 | Redfield et al. (1963) |
| $\eta$ | Zooplankton efficiency | 0.75 | Fasham et al. (1990) |
| $\gamma$ ($s^{-1}$) | Zooplankton growth | $1.157 \times 10^{-5}$ | Fasham et al. (1990) |
| $k_P$ (μmol N $dm^{-3}$) | Grazing half-saturation | 1.0 | Fasham et al. (1990) |
| $\delta$ ($s^{-1}$) | Zooplankton mortality | $1.730 \times 10^{-6}$ | Fasham et al. (1990) |
| $\alpha$ | Degradation fraction | 0.33 | Crispi et al. (2006) |
| $r$ ($s^{-1}$) | Detritus remineralization rate | $1.18 \times 10^{-6}$ | Crispi et al. (2002) |
| $w_D$ (cm $s^{-1}$) | Detritus sinking velocity | $5.8 \times 10^{-3}$ | Crispi et al. (2002) |
| $K_H$ ($cm^4$ $s^{-1}$) | Horizontal turbulent diffusion | $1.5 \times 10^{18}$ | Crispi et al. (2006) |
| $K_V$ ($cm^2$ $s^{-1}$) | Vertical turbulent diffusion | 3.6 | This work |
| $n_C$ | Cox turbulence iteration number | 10 | Crispi et al. (2006) |
| $\alpha_B$ ($s^{-1}$) | Newtonian restoration time | $1.157 \times 10^{-5}$ | Crispi et al. (2006) |

### 2.3. Initial biochemical conditions

The phytoplankton is initialized using a typical summer profile. It starts from the average of the stations measured by Berland et al. (1988, see Fig. 5) in the Balearic Sea, Ionian Sea, and Levantine Basin. After averaging these three chlorophyll vertical distributions, a transformation of 0.05 for estimating the chlorophyll to biomass transformation has been adopted, as shown in Fig. 1, inner panel. At the same level in Fig. 1, zooplankton is initialized at one-ninth of the phytoplankton value, which is in line with the oceanic zooplanktonic biomass of approximately 12–15% of the total content of phytoplankton. Detritus is set till 100 m depth, according to Coste et al. (1988), to the particulate matter measured in the inflowing water: 0.5 μmol N $dm^{-3}$.

The mean nitrate levels under summer conditions are extracted from the MEDAR climatology (Manca et al., 2004). The data under areas DS4, DJ7, and DH3 are selected and averaged, corresponding to the regions in which data on phytoplankton were acquired. The interpolation on the depths of the model is reported in Fig. 1, large panel, as well as in the original regional profiles in the three areas. This full line profile initializes nitrate variable for all the regions of the Mediterranean basin: it is higher compared with the mean values of the Eastern Mediterranean in the intermediate water, ranging from 300 to 1000 m, while the content in the Western Mediterranean is underestimated because of the low values in the deeper water, approximately lower by 50% than the average concentrations in the deep regions.

### 2.4. Atlantic and marginal seas reservoirs

Attention was paid to the influence of the Atlantic and the marginal seas, northern Adriatic and Aegean, by means of boundary conditions to the pelagic Mediterranean.

Initialization and restoration to the same values of the Atlantic Ocean are performed. The station data are selected from the ATLANTIS II cruise report (Osborne et al., 1992). The reference latitude is 36.5°N and the longitude of these casts range from 9.5 to 8°W. The values are linearly interpolated on the discretized levels of the model.

For the northern Adriatic Sea, a marginal sea is introduced, giving rise to reasonable concentrations along the Italian coast. This area also maintains the mean biochemical climatological values, averaging the main effects of the rivers, whose sources and shelf processes are consistently given at the chosen 43°N model interface. As a matter of fact, these climatological profiles maintain a strong stability in the water column during the seasonal cycles (Zavatarelli et al., 1998; particularly see Fig. 11, which shows the seasonal vertical profiles in the Middle Adriatic). For this purpose, a central area of the Adriatic Sea northerly than 43°N is averaged. All the casts between Rimini–Pula and Vieste–Split transects are selected, but only if deeper than 80 m. The nitrate profile is interpolated according to the level depths in the model.

For the northern Aegean Sea, the area including the Cretan Sea northerly than 38°N is considered starting from measured profiles

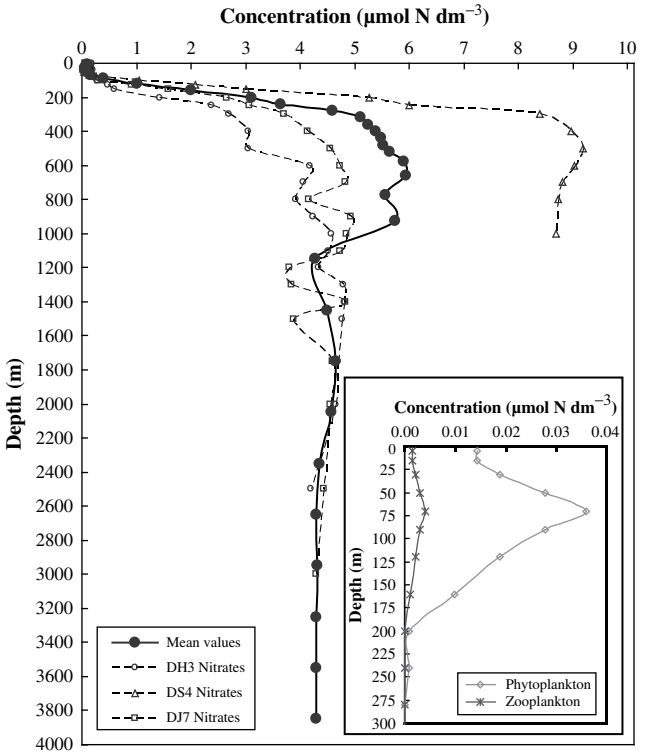


**Fig. 1.** The homogeneous initial conditions of inorganic nitrogen (full line) and the original summer nitrate profiles in the three areas of the Mediterranean (dashed lines) are shown. The initial conditions of summer phytoplankton (stars) and zooplankton (diamonds) are shown in the inner frame.

(McGill, 1970). In this northern marginal area, it is convenient to take into account the fluxes through the Aegean, in view of studies about climatic changes in the pelagic southern and deeper areas (Balopoulos et al., 1997).

The other biochemical variables relax in Newtonian restoring methodology to the respective initial profiles. The source term in each of the three areas for each biochemical tracer, $B$, with initial conditions, $B_0$, is given by:

$$\Delta B = \alpha_B(B - B_0) \tag{16}$$

These descriptions of the marginal seas solve two main important nutrient sources of the Eastern Mediterranean, namely, Po River and Bosphorus. Further inputs to the Eastern Mediterranean euphotic zone, such as Nile River and atmospheric load, are considered in the refinement of the model given in Section 2.5.

### 2.5. Atmospheric and terrestrial loads

Atmospheric loads are summarized in Fig. 2. According to Guerzoni et al. (1999), three surface areas with different total nitrogen are considered: Western, Central, and Eastern Mediterranean. The first area gives an amount of $12.54 \times 10^{-8}$ μmol N dm$^{-3}$ s$^{-1}$. The central area contributes $9.93 \times 10^{-8}$ μmol N dm$^{-3}$ s$^{-1}$. The eastern basin loads $8.63 \times 10^{-8}$ μmol N dm$^{-3}$ s$^{-1}$. The uncertainties are approximately 25% of these averages, well in line with global scale oceanic estimations (Galloway et al., 2004).

The different run configurations are also reported in the scheme: the reference run (RRUN) has been performed without any inputs (either terrestrial or atmospheric); the inorganic input run (IRUN) takes account of the 100% input in the surficial inorganic nitrogen compartment; finally in the fractionated run (FRUN), inputs are divided between inorganic nitrogen (50%) and organic nitrogen (50%), contributing to surface detritus.

The terrestrial loads considered here are in the Rhone and in the Nile areas. These inputs are assigned on the basis of yearly average of nitrogen loads for the Gulf of Lions (Durrieu de Madron et al., 2001) and Nile Delta (Hamza, 2001). The total nitrogen loads are transformed into fluxes and added continuously over time at the first 10 m of the shelf interested by the river discharges. Rhone River discharges, in an area of approximately 9000 km$^2$, $3.18 \times 10^{-6}$ μmol N dm$^{-3}$ s$^{-1}$. Nile River contributes $6.82 \times 10^{-7}$ μmol N dm$^{-3}$ s$^{-1}$ in the Delta region of approximately 15,900 km$^2$. Freshwater is not added and dilution effects are taken into account through the surface climatological restoration of the salinity.

### 2.6. Chlorophyll equivalent for surface biomass

Till now the ecosystem model has been based on biomass expressed in nitrogen units. As above-mentioned, the N:C ratio inside the plankton is taken as fixed and as equal to the Redfield ratio, $R_{NC}$. The conversion into chlorophyll units requires the knowledge of the amount of carbon with respect to the chlorophyll inside the cell. This type of conversion can be either a statistical, which is chosen in the 20 m upper layer, or a phenomenological one, which is used from 20 m down.

In the following, surface chlorophyll concentration, from the surface to a depth of 20 m, is achieved by applying the statistical expression as obtained by Cloern et al. (1995) who studied mainly diatom cultures. This expression is a function of temperature, irradiance at surface, and nitrogen availability:

$$\frac{R_{NC}}{12}\frac{\mathrm{Chl}}{P} = 0.003 + 0.0154\, e^{0.05T}\, e^{-0.059\frac{I_0(t)(1-e^{-k_z z_o})}{k_z z_o}} N_f(N) \tag{17}$$

In Eq. (16) Chl and $P$ are, respectively, the chlorophyll (mg Chl m$^{-3}$) and model's biomass concentrations (μmol N dm$^{-3}$), converted from nitrogen units into carbon by means of the $R_{NC}$ ratio and the carbon atomic weight; $T$ is the potential temperature (°C); $k_z$ is the light extinction coefficient (cm$^{-1}$); and $z_o$ is the upper layer thickness.

$I_0(t)$ represents radiation available for photosynthesis at surface, expressed in Langley day$^{-1}$, and it has been calculated on a daily basis, according to Sverdrup et al. (1942).

$$I_0(t) = (1 - \mathrm{ref})(1 - \mathrm{lw})\left[600 - 340\cos\left(\frac{2\pi(\mathrm{day} + 10)}{365}\right)\right] \tag{18}$$

where ref represents for reflected light equal to 0.15 and lw means long-wave radiation equal to 0.55. The term day in Eq. (18) corresponds to a vector of 365 days. The light parameters, 600 and 340,

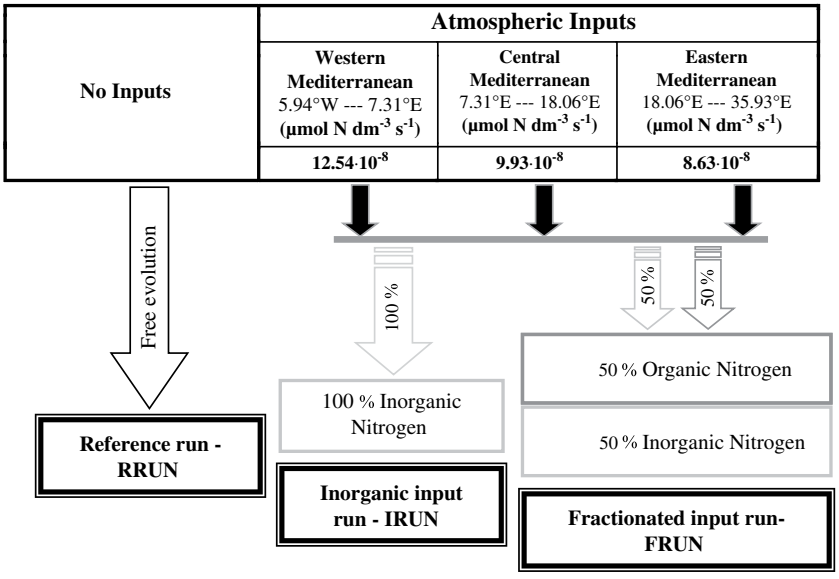


**Fig. 2.** Schematics of the atmospheric inputs and relative repartition among ecological compartments. Both IRUN and FRUN are loaded with nutrient discharges from rivers.

have been converted from Langley day$^{-1}$ to mol quanta day$^{-1}$ m$^{-2}$ in order to be applied in Eq. (17).

The model's chlorophyll concentrations in deeper layers are obtained after transformation from nitrogen units to carbon content, by means of the Redfield ratio and the carbon atomic weight, and afterwards from carbon to chlorophyll, by means of Chl:C ratios, which differ in the Western and Eastern Mediterranean.

For the Western Mediterranean, Jacques et al. (1973) estimated integrated values of approximately 67.0 mg Chl m$^{-2}$ in the 200 m upper layer, where the estimation of the phytoplankton biomass is 3.83 g C m$^{-2}$ (Nival et al., 1975); therefore, the resulting Chl:C ratio in the Western Mediterranean is 0.0175.

In the Eastern Mediterranean, the integrated chlorophyll in the Aegean Sea in winter from surface to 1.5 of the critical depth, approximately 90 m, is 18.8 mg Chl m$^{-2}$ (Vidussi et al., 2001) and, in the same season, Siokou-Frangou et al. (2002) measured 1.89 g C m$^{-2}$ as average value of chlorophyll of the total autotrophs in the upper 100 m; from these data, the Chl:C ratio in the Western Mediterranean is 0.0073.

## 3. Results

### 3.1. Vertical chlorophyll profiles in the eastern basin

Vertical chlorophyll profiles, averaged between 33 and 35°N, for RRUN, IRUN and FRUN are shown in the Eastern Mediterranean (Fig. 3) every 10 days, starting from the 1st of September. After approximately 1 month deep chlorophyll maximum (DCM) can be observed at 90 m depth in Fig. 3a, reaching 0.30 mg Chl m$^{-3}$. The surficial input effects can be recognized in the first 30 m, as seen in Fig. 3b, where the absolute values increase by approximately 50% with respect to RRUN. However, there is no evident effect on the DCM at 90 m depth. Fig. 3b and c appear very similar; however, an accurate analysis reveals that at the surface, IRUN shows a greater chlorophyll signal than do FRUN, while it is quite the opposite at the DCM.

The 3-D biogeochemical model, even simulating a generic food chain, has the main factors suitable for reproducing adequately the chlorophyll vertical structure. This sensitivity experiment shows that atmospheric nitrate inputs in different forms do not significantly affect the biomass in terms of chlorophyll at the DCM, but can change considerably the responses at the surface layers.

In these oligotrophic waters, DCM is a combined effect of light and nutrient limitations, the former increasing and the latter decreasing with depth. This indicates that DCM responds dynamically to the ambient solicitations: decrease in light intensity, vertical turbulent diffusion, and nutrient availability.

### 3.2. Evolution in the western and in the eastern basins

The evolutions of inorganic nitrogen, plankton – here the sum of nitrogen content of phytoplankton and zooplankton – and detritus, in western basin expressed in percentages of the total nitrogen content, are shown in Fig. 4. The score of the inorganic nitrogen is more than 70% in the case of absence of atmospheric input (Fig. 4a). This is an oligotrophic condition, with approximately 15% of the total content found in plankton and approximately half this quantity in detritus.

Considering atmospheric inputs in Fig. 4b and c, the inorganic nitrogen percentage falls below 70% with a quota of input by phytoplankton higher than 20%. This higher phytoplankton concentration with respect to the atmospheric inputs is due to the increase of inorganic nitrogen in euphotic zones of the sea; inducing an higher nutrient limitation factor, $N_f(N)$ in Eq. (12), which gives faster growth responses for the plankton.

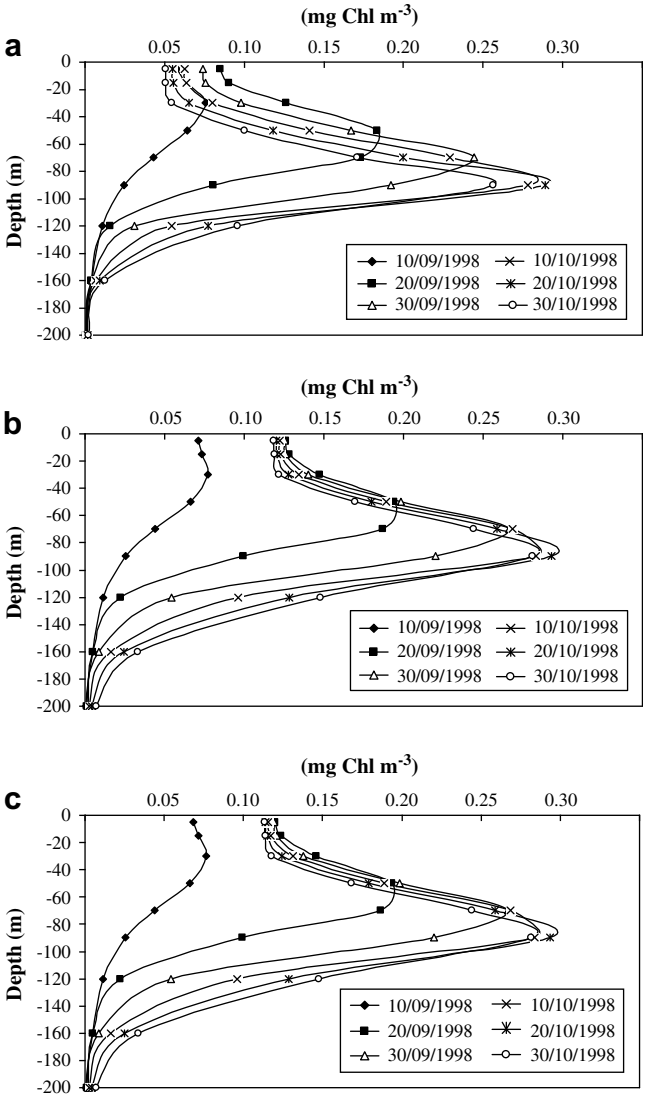


**Fig. 3.** Vertical chlorophyll profiles at 33–35°N in the Eastern Mediterranean, showing RRUN (a), IRUN (b) and FRUN (c). The period spans from the beginning of September to the end of October during the first simulation year.

These results match with those obtained by a multi-nutrient approach (Crise et al., 2003). Both in the Western and in the Eastern Mediterranean (not shown), the vertically integrated inorganic nitrogen accounts for approximately 80% of the total nitrogen for the two different atmospheric inputs. The more oligotrophic areas utilize higher quotas of their total nitrogen in the biogenic fraction. The detritus consumes 7–8% of the total nitrogen, and the rest is used by the fractionated plankton components.

### 3.3. Total nitrogen content in the surface and intermediate layers

The evolution of total nitrogen content in the Mediterranean basin is shown in Fig. 5 for the three runs, RRUN, IRUN and FRUN. The simulations span, as before, from the 1st of September to the 3rd of November.

The total nitrogen loss for the case of no input run is high, approximately 1300 $\times$ 10$^3$ ton N year$^{-1}$. This imbalance is due to the effects at Gibraltar of the Atlantic water inflow and outflow of the nutrient-rich Levantine water, without any terrestrial or atmospheric inputs.

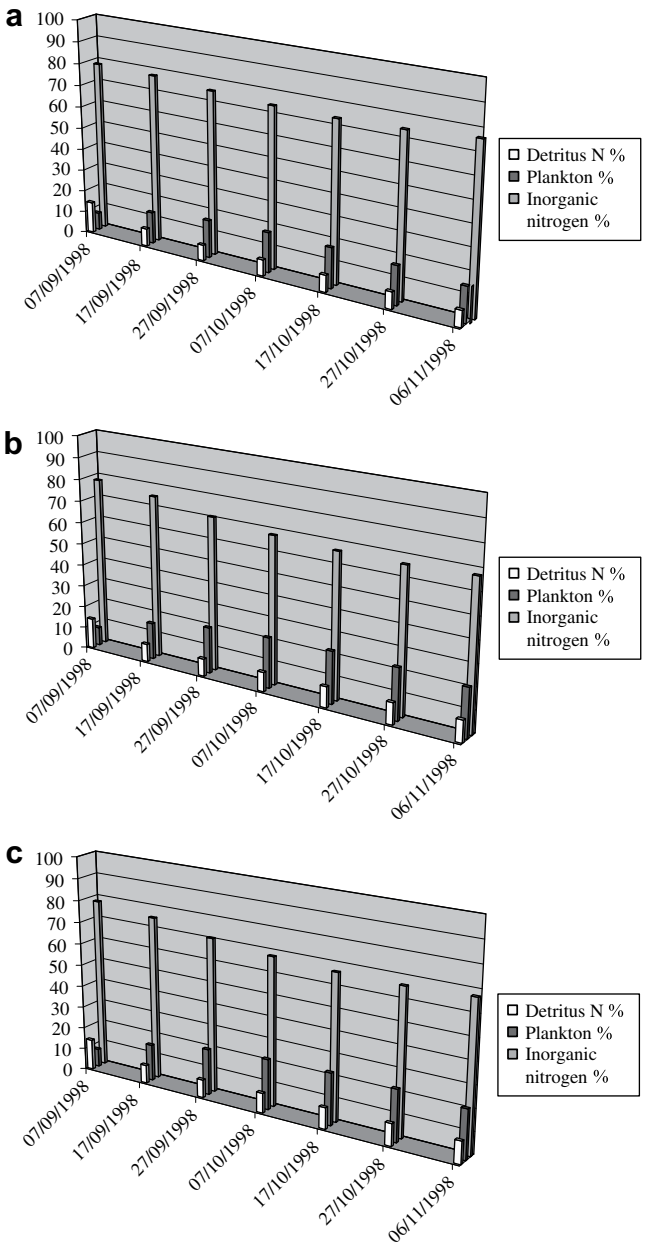


**Fig. 4.** The contents of detritus, plankton (phytoplankton plus zooplankton) and inorganic nitrogen in the 0–180 m surface layer of the Western Mediterranean. Percentages are shown for the three runs RRUN (a), IRUN (b), and FRUN (c).

As a matter of fact, the fluxes obtained through various methods with yearly average statistical approach, i.e. inflowing nutrients minus outflowing ones, give estimations from approximately $2500 \times 10^3$ ton N year$^{-1}$ (Lacombe, 1971; Bethoux, 1979) to half this value (Sarmiento et al., 1988; Bryden and Kinder, 1991; Harzallah et al., 1993). Thus, the value obtained using NPZD Mediterranean model is consistently in line with information and elaborations from existing data sets.

Whereas for IRUN and for FRUN the nitrogen losses are much lower, approximately $28–30 \times 10^3$ ton N year$^{-1}$. In fact, the two simulations with atmospheric inputs, showing very close values, seem to reach a nearly flat trend in nitrogen content.

Certainly, the limited length of the simulations can affect these results. For giving a long-term insight into the method, the third run, FRUN, with atmospheric loads fractionated into inorganic and

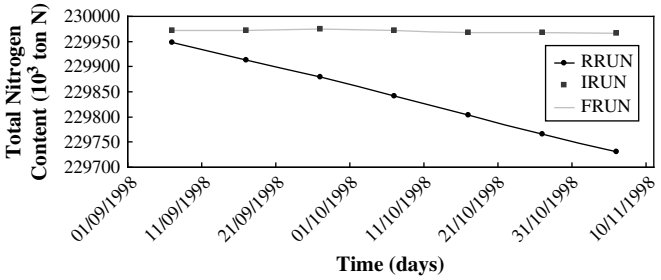


**Fig. 5.** Total nitrogen of the Mediterranean, comparing the three simulations RRUN, IRUN, and FRUN in the first 70 days.

organic part, is considered in the following results given in Figs. 6–9. This atmospheric input closely resembles experimental evidences in the measurement stations extrapolated at a basin scale. Decadal simulation spanning 33 years and 8 months is performed for estimating the budget and content trends.

The evolution of the euphotic zones of the Western and Eastern Mediterranean is shown in Fig. 6a, representing the total nitrogen contents in the upper layer in the western and eastern basins, respectively. They are calculated by integrating the concentrations from the surface to the 180 m maximum depth. Averaging is performed by weighting with respect to the surfaces of the western and eastern basins.

Maxima and minima alternate at the yearly clock of the winter mixing, enriching the euphotic area, and of the summer stratification, exporting organic matter. The seasonal fluctuations are small but not negligible, relatively more important, approximately 10% of the mean value, in the Eastern Mediterranean.

The eastern basin total nitrogen content steeps with a lower temporal gradient, nearly at a quasi-equilibrium state. As a matter

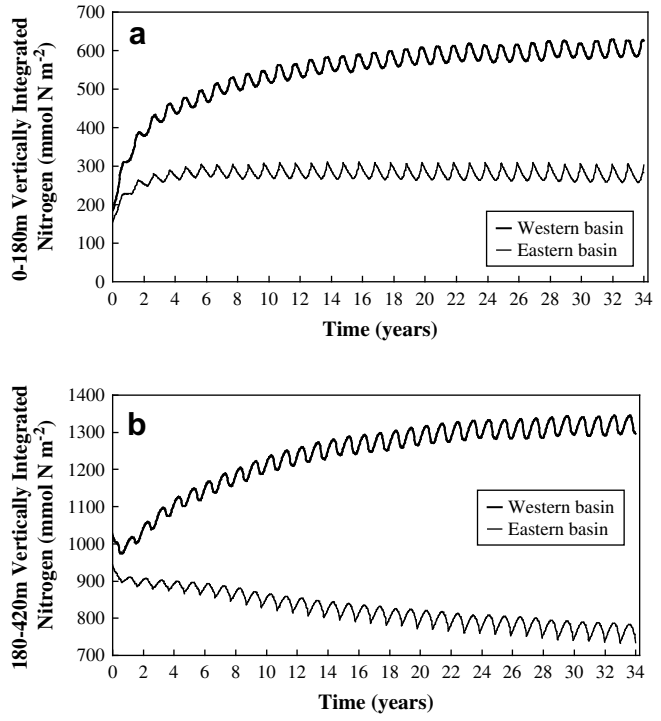


**Fig. 6.** Total nitrogen content in the upper 0–180 m layer (a) and in the intermediate 180–420 m layer (b), averaging FRUN in the western (thick line) and eastern (thin line) basins. The contents in the marginal sea reservoirs are excluded from the weighted averages.

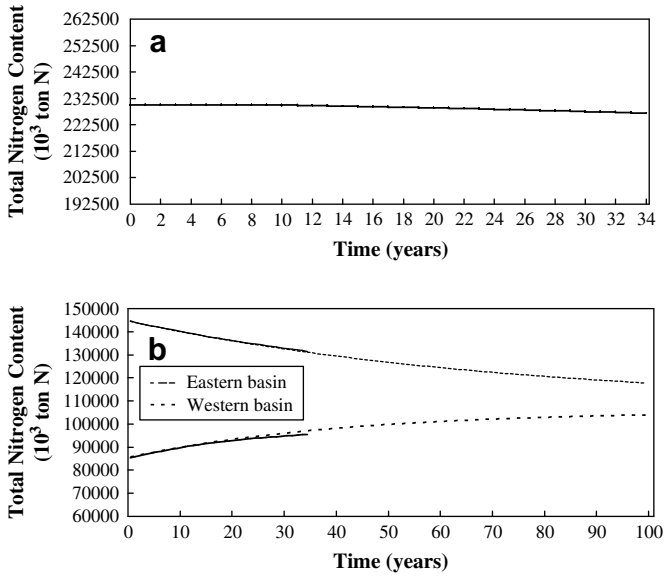


**Fig. 7.** Total nitrogen content of the Mediterranean (a) and sub-basin total nitrogen contents (b), considering 33 years and 8 months of the FRUN, are shown for the western (thick line) and eastern (thin line) basins. The optimal exponential evolutions in each basin are plotted with dashed lines.

of fact, the used initial profiles are taken from the phenomenology of samples taken in the Eastern Mediterranean, except for the DS4 Balearic station. The eastern basin contents of Fig. 6a, particularly summer minima, are close to the initial value, which for the reasons given above is closer to eastern climatology.

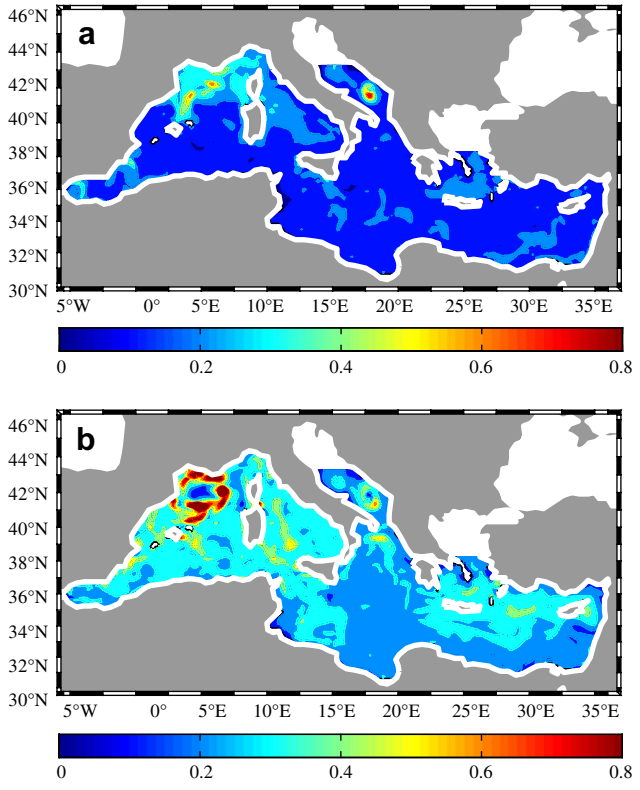


**Fig. 8.** Averaged surface chlorophyll concentrations (mg Chl $m^{-3}$) during January are shown in the first year (a) and in the 34th year (b) of the FRUN. The values in northern Adriatic Sea above 43°N and in northern Aegean Sea above 38°N are blank.

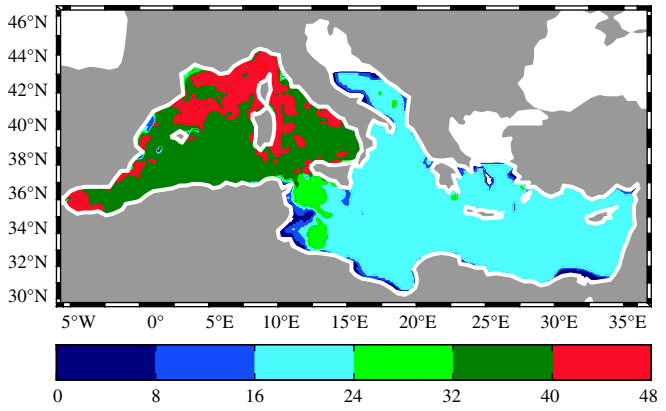

**Fig. 9.** Yearly vertically integrated chlorophyll (mg Chl $m^{-2}$) in the upper 0–180 m layer, considering the last 3 years of FRUN.

Dynamically, the FRUN simulation tends, after about a decade, to values higher than 600 mmol N $m^{-2}$ in the western basin, significantly higher than the 250 mmol N $m^{-2}$ reached on average in the eastern part. Thus, the total content in the Western Mediterranean is more than double in the long run (Fig. 6a).

The observed evolution is due only to the ecosystem response to currents, wind stress and temperature, because all the other chemical and biological conditions affecting growth are the same in all the regions of the Mediterranean.

In these two upper layers the biogeochemical processes have a distinct role. Phytoplankton growth, grazing and remineralization trap chemical energy in these upper layers, reaching total nitrogen content higher than the ubiquitous initial conditions of the system. This is not inconsistent from an evolutionary point of view; in reality the initial phytoplankton is a typical summer biomass and also the detritus starts from low average values. Thus, in Fig. 6a the western basin gains significantly in total nitrogen content, tending toward the formation of a nutrient enriched environment. This mesotrophic state is also attained because Western Mediterranean experiences upwelling processes and convection.

This behavior emerges in a striking manner from evolutions in the same FRUN simulation of the intermediate layers from 180 to 420 m (Fig. 6b). Extreme values alternate with the recurrent yearly period, but reversing the maxima in Fig. 6a with minima here, and vice versa.

Starting from similar values of the total content, due to major development of the shelf in the Eastern Mediterranean than in the Western one, the response of the two basins is different. In this case, we see that longer intervals, approximately two or three decades, are necessary for reaching stable values.

In Fig. 6b, the increase in the total content of the Western Mediterranean is well depicted by the remineralization of the detritus fraction of the mesotrophic upper layer, sinking from euphotic areas down into the intermediate waters. There is a deviation from the initial conditions that are typical for the central and eastern basin, but not representative of the conditions in the Western Mediterranean. This is well evident from the database existent for the Mediterranean Sea in terms of nitrate (MEDAR Group, 2002): considering their climatological horizontal map at 300 m, at the middle of the chosen layer, high concentrations are recovered and the integrated values are close to those given in Fig. 6b.

The decrease in the total content of the eastern basin (Fig. 6b) is consistent with the inorganic nitrogen initial profile. The latter deviates from the oligotrophic values of the eastern stations by the DS4 Balearic station. The biogeochemical model recovers after few

decades of more oligotrophic conditions in this intermediate layer, combining the minor remineralization of the upper oligotrophic layers and the outflow from the Sicily Strait of the excess content of inorganic nitrogen. The analysis of the above-mentioned climatological map gives good comparison in terms of both zonal gradients and absolute integrated values.

### 3.4. Total content in the overall Mediterranean and sub-basins

Fig. 7a shows the evolution of the total nitrogen content in the Mediterranean basin, considering the fractionated input FRUN for the long evolution.

After a nearly flat evolution, the total nitrogen content decreases during the last few years of the simulation. This behavior is understandable in terms of biological activity. The growth of phytoplankton in late winter–early spring, and consequent production of detritus, after remineralization, fertilizes outflow from the intermediate layers, decreasing net inputs from Gibraltar Strait.

The average total nitrate loss in the final years is approximately $150 \times 10^3$ ton N year$^{-1}$. This is well in line with the result obtained with the 2-month simulation in Fig. 5 and it indicates that the basin fluxes are stabilizing around their annual dynamical cycles, reinforcing the conclusion of dynamical stability of the total nitrogen content.

The evolutions of the total nitrogen in the two sub-basins are shown in Fig. 7b, with the best exponential fits.

The FRUN results are not sufficient to develop fully steady states because of the contribution of the deeper layer to the accumulation of nitrogen, which is expected in the Western Mediterranean, and the decrease in overall nitrogen, i.e. oligotrophism, in the Eastern Mediterranean.

The final best-fit equilibria are very dissimilar from each other. A final total bulk content in the Western Mediterranean is found to be $105 \times 10^6$ ton N. Considering a total volume ($12.9 \times 10^5$ km$^3$), average resulting concentration is approximately 5.8 μmol N dm$^{-3}$. The response of the Western Mediterranean is fast, with respect to geological times, and is attained in 40 years.

The condition in the eastern basin is different because the equilibrium value of $108 \times 10^6$ ton N is diluted in a larger volume ($24.6 \times 10^5$ km$^3$). This gives an average concentration of 3.1 μmol N dm$^{-3}$. The response time in this case is longer and reaches 72 years. This result is of the same order of the residence time of 124 years obtained by Roether and Schlitzer (1991) for deep-water renewal using tracer data and marks the difference between the biogeochemical cycles and the physical processes, with the former quicker than the latter.

The core outcome of this numerical exercise is that the biogeochemical nitrogen cycle is strongly affected by the general circulation in the Mediterranean. The obtained oligotrophy is consistent with the known phenomenology of the Eastern Mediterranean because the Adriatic rivers, the Central Europe discharge through Bosphorus, the major Nile River, and the average atmospheric loads are all taken into account. The Western Mediterranean attains quite good values, with some persistent loss at Gibraltar. This suggests that some data are lacking in terms of anthropogenic diffuse input of the central and northwestern coastal systems.

### 3.5. Response of the chlorophyll at surface

The average chlorophyll concentration map at the surface (0–20 m) during January of the first year of the FRUN simulation is shown in Fig 8a.

This map represents the high chlorophyll signal corresponding to the well-known permanent cyclonic circulation in the Gulf of Lions and the structures in the Tyrrhenian Sea and Ligurian Basin. A pronounced and concentrated feature supported by weak cyclonic circulation characterizes South Adriatic. The eastern basin shows lower chlorophyll values in accordance with its typical oligotrophic environment. Higher chlorophyll is present in the northern coast of Crete island due to upwelling, according to the stream function, not shown.

The same chlorophyll field is represented in Fig. 8b, but this plate refers to the situation after 33 years of free evolution of the ecosystem. The structures in Fig. 8a in the Gulf of Lions and Balearic Sea appear to increase and intensify around the cyclonic area. There are also increasing signals of the zonal gradients across the entire Mediterranean. New features emerge particularly in the central Tyrrhenian Sea and along the Calabrian Shelf. The effects of the cyclonic area aside Crete are more evident.

From a quantitative point of view, the maxima in the western basin are well in the range of the experimental data in that area during late winter (Berland et al., 1973). These give 0.5 mg Chl m$^{-3}$ in accordance with the values of 0.5–0.7 mg Chl m$^{-3}$ reached finally by the model. In the eastern basin, the oligotrophic range of 0.1–0.2 mg Chl m$^{-3}$ is hardly overcome in this winter month, as confirmed by the data taken during the same season in the Levantine Basin, Israeli pelagic station and southern region (Azov, 1986; Berman et al., 1986).

### 3.6. Integrated biomass in the euphotic zone

In Fig. 9 the yearly vertically integrated chlorophyll is shown as obtained after averaging model's results of the last three simulation years. The richer area is the northwestern Mediterranean, with values above 40 mg Chl m$^{-2}$; in other smaller areas of the Western Mediterranean, like Alboran Sea, Balearic Sea and Tyrrhenian Sea, similar values are also obtained. The yearly vertically integrated chlorophyll decreases slightly in the southern part of the Western Mediterranean and, more evidently, easterly. In the Eastern Mediterranean the chlorophyll values present a homogeneous signal and are generally below 24 mg Chl m$^{-2}$.

The model's sub-basin results are compared in Table 2 with the yearly vertically integrated chlorophyll averaged in the Western Mediterranean from 10 regional profiles and in the Eastern Mediterranean, including Sicily Channel, from 13 ones (Manca et al., 2004; website, http://doga.ogs.trieste.it/medar/). The model's standard errors due to the atmospheric input uncertainties are calculated as averages of the last 3 years of three scenarios, respectively, loaded with 75, 100 and 125% of the FRUN atmospheric inputs.

The data averages characterize abundance of total chlorophyll in the euphotic zone in the Western Mediterranean, consequence of the mesotrophic conditions that induce an intermediate regime and biomass. The Eastern Mediterranean chlorophyll consists in lower integrated biomass, approximatively half than that contained in the western sub-basin, reflecting the oligotrophic characteristics. Model's results give a similar situation confirming higher chlorophyll in the western basin and lower in the eastern basin. The slight underestimation of the simulated vertically integrated chlorophyll can be also due to other numerical uncertainties and minor shelf contributions in northern, generally richer in chlorophyll, areas.

Standard errors inferred through experimental data give a very large error in the western basin and lower one, less than one-third, in the eastern basin. These errors reflect the various physical, chemical and biological variabilities in both basins. The model's errors are lower and still of the same order of magnitude than experimental ones; anyway, the atmospheric loads are important but not unique to determine the model's errors and some of these uncertainties remain still to be realistically evaluated in terms of the physical–chemical variabilities and the ranges of the parameters.

**Table 2**
Estimated averages and standard errors calculated from the experimental chlorophyll profiles and from FRUN in Western and Eastern Mediterranean.

| Estimated biomass indicators | Western Mediterranean ($mg\ Chl\ m^{-2}$) | Eastern Mediterranean ($mg\ Chl\ m^{-2}$) |
|---|---|---|
| Integrated in situ chlorophyll | 41.0 | 24.1 |
| In situ chlorophyll error | 6.0 | 1.9 |
| Integrated FRUN chlorophyll[a] | 37.0 | 17.5 |
| FRUN chlorophyll error[b] | 4.9 | 1.3 |

[a] Estimated averages in the last 3 years of the FRUN simulation.
[b] Estimated errors in the last 3 years of the FRUN simulation, due to atmospheric loads only.

## 4. Conclusions

The main conclusion of this study is that principal river inputs and atmospheric loads are required in order to preserve total nitrogen content of the Mediterranean Sea. Thus, a synthetic approach, combining field data and theoretical knowledge, forms the basis of a proper long-term evolution of the biogeochemistry following the variability of the exchanges at the main Straits. This numerical exercise is affected by uncertainties of the atmospheric loads, but it is worth noting that new estimations based upon recent data, from independent sources, are in line with the ones considered as inputs in this study (Kouvarakis et al., 2001). The particulate matter, as measured by Coste et al. (1988), is significant in the overall budget as included in the model as independent detritus source at Gibraltar.

Total modelled nitrogen content in the Mediterranean Sea is very stable, showing small losses of approximately $150 \times 10^3$ ton N $year^{-1}$. This residual imbalance is probably attributable to further diffused nitrogen terrestrial discharges along the central and the northwestern coasts, not taken into account in the model.

When euphotic layers are analyzed as subsystems, the different behaviors of the Western and Eastern Mediterranean emerge. The western basin reaches in the long run quite a high nitrogen content, more than 600 mmol N $m^{-2}$, with respect to the low eastern content, less than 250 mmol N $m^{-2}$. The interpretation relies upon the combination of the negative thermohaline circulation with the biogenic fertilization of the intermediate layers: the westward interior flux permits significant total nitrogen impoverishment in the Eastern Mediterranean, which is relatively less important in the Western Mediterranean.

The spatial chlorophyll distribution, as vertically integrated in the euphotic zone at the end of the long-term simulation, can be considered a reasonable approximation with respect to data knowledge. The biomass in the Western Mediterranean is approximately twice that in the eastern basin, confirming, also in these deeper layers, the surficial trophic gradients well recognized by satellite maps.

## Acknowledgements

This study has been supported by EC contract MFSTEP/EVK3-CT-2002-00075.

The preliminary results of this article have been presented at the 8th International Marine Environmental Modelling Seminar, Helsinki Finland, August 23–25, 2005.

The authors also thank the Referees and Editor for their helpful suggestions and text comments.

## References

Azov, Y., 1986. Seasonal patterns of phytoplankton productivity and abundance in nearshore oligotrophic waters of the Levant basin (Mediterranean). Journal of Plankton Research 8 (1), 41–53.

Balopoulos, E., Varnavas, S., Monaco, A., Price, N.B., Collins, M.B., Kotsovinos, N., Matsoukis, P., Dermissis, V., Apostolopoulou, M., 1997. Hydrodynamics and biogeochemical fluxes in the straits of the Cretan Arc (Aegean Sea, Eastern Mediterranean Basin). In: Lipiatou, E. (Ed.), Interdisciplinary Research in the Mediterranean Sea, Luxembourg, EUR 17787 EN, pp. 93–125.

Berland, B., Bonin, D., Coste, B., Maestrini, S., Minas, H.J., 1973. Influence des conditions hivernales sur les productions phyto- et zooplanctoniques en Méditerranée Nord-Occidentale. III. Caractérisation des eaux de surface au moyen de cultures d'algues. Marine Biology 23, 267–274.

Berland, B.R., Benzhitski, A.G., Burlakova, Z.P., Georgieva, L.V., Izmestieva, M.A., Kholodov, V.I., Maestrini, S.Y., 1988. Conditions hydrologiques estivales en Méditerranée, repartition du phytoplancton et de la matière organique. Oceanologica Acta 11 (SP), 163–177.

Berman, T., Azov, Y., Schneller, A., Walline, P., Townsend, D.W., 1986. Extent, transparency, and phytoplankton distribution of the neritic waters overlying the Israeli coastal shelf. Oceanologica Acta 9, 439–447.

Bethoux, J.P., 1979. Budgets of the Mediterranean Sea. Their dependence on the local climate and on the characteristics of the Atlantic waters. Oceanologica Acta 2 (2), 157–163.

Bethoux, J.P., Morin, P., Madec, C., Gentili, B., 1992. Phosphorus and nitrogen behaviour in the Mediterranean Sea. Deep-Sea Research 29 (9), 1641–1654.

Bryden, H., Kinder, T.H., 1991. Steady two-layer exchange through the Strait of Gibraltar. Deep-Sea Research 38 (Suppl. 1), 445–463.

Carrada, G., Hopkins, T., Jeftié, L.J., Morcos, S. (Eds.), 1983. Quantitative Analysis and Simulation of Mediterranean Coastal Ecosystems: the Gulf of Naples, a Case Study. UNESCO Reports in Marine Sciences, vol. 20, p. 158.

Cloern, J.E., Grenz, C., Vidergar-Lucas, L., 1995. An empirical model of the phytoplankton chlorophyll:carbon ratio – the conversion factor between productivity and growth rate. Limnology and Oceanography 40 (7), 1313–1321.

Coste, B., Le Corre, P., Minas, H.J., 1988. Re-evaluation of the nutrient exchanges in the Strait of Gibraltar. Deep-Sea Research 35, 767–775.

Crise, A., Crispi, G., Pacciaroni, M., 2003. CD-ROM with 3D Eco-hydrodynamical Model Outputs of Downward Fluxes and Model Code (MOM-based with Coupled Biological Submodel). ADIOS/EVK3–CT–2000–00034 Deliverable, D40–M32.

Crispi, G., Crise, A., Solidoro, C., 2002. Coupled Mediterranean ecomodel of the phosphorus and nitrogen cycles. Journal of Marine Systems 33–34, 497–521.

Crispi, G., Mosetti, R., Solidoro, C., Crise, A., 2001. Nutrients cycling in Mediterranean basins: the role of the biological pump in the trophic regime. Ecological Modelling 138 (1–3), 101–114.

Crispi, G., Pacciaroni, M., Viezzoli, D., 2006. Simulating biomass assimilation in a Mediterranean ecosystem model using SOFA: setup and identical twin experiments. Ocean Science 2 (2), 123–136.

Demirov, E., Pinardi, N., 2002. Simulation of the Mediterranean Sea circulation from 1979 to 1993: part I. The interannual variability. Journal of Marine Systems 33–34, 23–50.

Dugdale, R.C., Goering, J.J., 1967. Uptake of new and regenerated forms of nitrogen in primary productivity. Limnology and Oceanography 12 (2), 196–206.

Dugdale, R.C., Wilkerson, F.P., 1988. Nutrient sources and primary production in the Eastern Mediterranean. Oceanologica Acta 11 (SP), 179–184.

Durrieu de Madron, X., Denis, L., Diaz, F., Garcia, N., Guieu, C., Grenz, C., Loÿe-Pilot, M.D., Ludwig, W., Moutin, T., Raimbault, P., 2001. Freshwater and Freshwater Nutrient Sources Gulf of Lions, France LOICZ int. Rep., Available from: http://data.ecology.su.se.

Eppley, R.W., Rogers, J.N., McCarthy, J.J., 1969. Half-saturation constants for uptake of nitrate and ammonium by marine phytoplankton. Limnology and Oceanography 14 (6), 912–920.

Fasham, M.J.R., Duklow, H.W., McKelvie, S.M., 1990. A nitrogen-based model of plankton dynamics in the oceanic mixed layer. Journal of Marine Research 48, 591–639.

Galloway, J.N., Dentener, F.J., Capone, D.G., Boyer, E.W., Howarth, R.W., Seitzinger, S.P., Asner, G.P., Cleveland, C.C., Green, P.A., Holland, E.A., Karl, D.M., Michaels, A.F., Porter, J.H., Townsend, A.R., Vörösmarty, C.J., 2004. Nitrogen cycles: past, present, and future. Biogeochemistry 70 (2), 153–226.

Guerzoni, S., Chester, R., Dulac, F., Herut, B., Loye-Pilot, M.D., Measures, C., Migon, C., Molinaroli, E., Moulin, C., Rossini, P., Saydam, C., Soudine, A., Ziveri, P., 1999. The role of atmospheric deposition in the biogeochemistry of the Mediterranean Sea. Progress in Oceanography 44 (1–3), 147–190.

Hamza, W., 2001. The Phenomenology of the Mediterranean Egyptian Coastal Area MFSPP int. rep., Available from: www.pml.ac.uk/ecomodels/oldpages/Egypt.htm.

Harzallah, A., Cadet, D.L., Crepon, M., 1993. Possible forcing effects of net evaporation, atmospheric pressure, and transients on water transports in the Mediterranean Sea. Journal of Geophysical Research 98 (C7), 12341–12350.

Jacques, G., Minas, H.J., Minas, M., Nival, P., 1973. Influence des conditions hivernales sur les productions phyto- et zooplanctoniques en Méditerranée Nord-Occidentale. II. Biomasse et production phytoplanctonique. Marine Biology 23 (4), 251–265.

Kouvarakis, G., Mihalopoulos, N., Tselepides, A., Starakakis, S., 2001. On the importance of atmospheric inputs of inorganic nitrogen species on the productivity of the eastern Mediterranean Sea. Global Biogeochemical Cycles 15 (4), 805–817.

Lacombe, H., 1971. Le détroit de Gibraltar, océanographie physique. In: Notes et Mémoire du Service Géologique du Maroc, 31 (222 bis), pp. 111–146.

Manca, B., Burca, M., Giorgetti, A., Coatanoan, C., Garcia, M.-J., Iona, A., 2004. Physical and biochemical averaged vertical profiles in the Mediterranean

regions: an important tool to trace the climatology of water masses and to validate incoming data from operational oceanography. Journal of Marine Systems 48 (1–4), 83–116.
McGill, D.A., 1970. Mediterranean Sea Atlas – Distribution of Nutrient Chemical Properties. Woods Hole Oceanographic Institution, Woodshole, MA.
MEDAR Group, 2002. MEDATLAS/2002 Database. Mediterranean and Black Sea Database of Temperature, Salinity and Bio-chemical Parameters. Climatological Atlas. IFREMER Edition (4 CDROMs).
Nival, P., Nival, S., Thiriot, A., 1975. Influence des conditions hivernales sur les productions phyto- et zooplanctoniques en Méditerranée Nord-Occidentale. V. Biomasse et production zooplanctonique – relations phyto-zooplancton. Marine Biology 31 (3), 249–270.
Osborne, J., Swift, J., Flinchem, E.P., 1992. OceanAtlas for MacIntosh. National Science Foundation, Reference #92–29, 106 pp.
Pacanowski, R., Dixon, K., Rosati, A., 1991. The G.F.D.L. Modular Ocean Model Users Guide. GFDL Ocean Group Technical Report #2. NOAA/Geophysical Fluid Dynamics Laboratory, Princeton, NJ, 17 pp.
Redfield, A.C., Ketchum, B.H., Richards, F., 1963. The influence of sea water. In: Hill, M.N. (Ed.), The Sea, vol. 2. Interscience, New York, pp. 26–77.
Roether, W., Schlitzer, R., 1991. Eastern Mediterranean deep water renewal on the basis of chlorofluoromethane and tritium data. Dynamics of Atmospheres and Oceans 15, 333–354.
Roussenov, V., Stanev, E., Artale, V., Pinardi, N., 1995. A seasonal model of the Mediterranean Sea general circulation. Journal of Geophysical Research 100 (C7), 13515–13538.
Sakshaug, E., Andresen, K., Kiefer, D.A., 1989. A steady state description of growth and light absorption in the marine planktonic diatom *Skeletonema costatum*. Limnology and Oceanography 34 (1), 198–205.
Sarmiento, J.L., Herbert, T., Toggweiler, J.R., 1988. Mediterranean nutrient balance and episodes of anoxia. Global Biogeochemical Cycles 2 (4), 427–444.
Siokou-Frangou, I., Bianchi, M., Christaki, U., Christou, E.D., Giannakourou, A., Gotsis, O., Ignatiades, L., Pagou, K., Pitta, P., Psarra, S., Souvermezoglou, E., Van Wambeke, F., Zervakis, V., 2002. Carbon flow in the planktonic food web along a gradient of oligotrophy in the Aegean Sea (Mediterranean Sea). Journal of Marine Systems 33–34, 335–353.
Steele, J.H., 1962. Environmental control of photosynthesis in the sea. Limnology and Oceanography 7 (2), 137–150.
Sverdrup, H.U., Johnson, M.W., Fleming, R.H., 1942. The Oceans: Their Physics, Chemistry and General Biology. Prentice Hall, New York, 1087 pp.
Thingstad, T.F., Rassoulzadegan, F., 1995. Nutrient limitations, microbial food webs, and 'biological C-pumps': suggested interactions in a P-limited Mediterranean. Marine Ecology Progress Series 117, 299–306.
UNESCO, 1981. The practical salinity scale 1978 and the international equation of state of seawater 1980. In: Tenth Report of the Joint Panel on Oceanographic Tables and Standards. Sidney, B.C., Canada, 1–5 September 1980UNESCO Technical Papers in Marine Science, vol. 36, 25 pp.
Vidussi, F., Clausure, H., Manca, B.B., Luchetta, A., Marty, J.-C., 2001. Phytoplankton pigment distribution in relation to upper thermocline circulation in the eastern Mediterranean Sea during winter. Journal of Geophysical Research 106 (C9), 19939–19956.
Wu, P., Haines, K., 1996. Modeling the dispersal of Levantine intermediate water and its role in Mediterranean deep water formation. Journal of Geophysical Research 101 (C3), 6591–6607.
Zavatarelli, M., Raicich, F., Bregant, D., Russo, D., Artegiani, A., 1998. Climatological characteristics of the Adriatic Sea. Journal of Marine Systems 18 (1–3), 227–263.